

NUMERICAL STUDIES ON THE INFLUENCE OF AIR STAGING ON THE TEMPERATURE OF FLUE GAS AND EMISSION OF GASES IN THE COMBUSTION CHAMBER OF OP 230 BOILER

Bartłomiej Hernik^{*,1}, Katarzyna Jagodzińska¹, Dominik Matuszek²

¹ Institute of Power Engineering and Turbomachinery, Silesian University of Technology, Konarskiego 18, 44-100 Gliwice, Poland

² PGE Dystrybucja S.A., Garbarska 21A, 20-340 Lublin, Poland

The primary methods of reducing nitrogen oxides, despite the development of more advanced technologies, will continue to be the basis for NO_x reduction. This paper presents the results of multivariate numerical studies on the impact of air staging on the flue gas temperature and composition, as well as on NO_x emissions in a OP 230 boiler furnace. A numerical model of the furnace and the platen superheater was validated based on measurements using a 0-dimensional model of the boiler. Numerical simulations were performed using the ANSYS Workbench package. It is shown that changes in the distribution of air to OFA nozzles, the angle of the air outflow from the nozzles and the nozzle location involve a change in the flue gas temperature and in the volume of NO_x and CO emissions at the furnace outlet.

Keywords: combustion, CFD, emission, boiler, NO_x

1. INTRODUCTION

According to the European Union environmental policy and the Industrial Emissions Directive, air pollutant emissions from industrial installations, such as nitrogen oxides (NO_x), have to be reduced (Directive 2010/75/EU). NO_x emissions are reduced using combinations of primary and secondary methods. The main aim of primary technologies is to decrease the temperature in a furnace and minimize the intensity of contact between fuel particles and combustion air, while generating a fuel-rich zone where it is possible to reduce NO_x into N₂. Generally, primary methods of NO_x reduction can be categorized into air staging, fuel staging (reburning), low NO_x burners and flue gas recirculation (Hardy and Pawlak-Kruczek, 2017).

Air staging, also referred to as “two-stage combustion” or “overfire air” (OFA), is the simplest technique to maintain because it does not require complicated air duct modifications or control systems. In industrial conditions, air staging is usually combined with fuel staging, which enables better control over the combustion process and the boiler operating parameters, as well as an improvement in the heat transfer in the furnace. As a rule, air staging involves dividing the furnace along its height, usually) and the combustion process into zones differing in air concentration – a sub-stoichiometric combustion zone (primary zone) and an above-stoichiometric combustion zone (second firing zone). In the primary zone, due to oxygen

* Corresponding author, e-mail: bartlomiej.hernik@polsl.pl

deficiency, NO_x concentrations are reduced towards creation of HCN, NH_3 and other non-oxidised nitrogen compounds, while in the second firing zone fuel particles are burnt completely (Nussbaumer, 1997; Spliethoff et al., 1997).

Research on air staging has been carried out for many years for combustion of fossil fuels and biomass (Buchmayr et al., 2016; Carroll et al., 2015; Khodaei et al., 2017; Kuang et al., 2013). Numerous experiments and numerical analyses have been performed for large-scale industrial boilers, mainly for pulverized-fuel (PF) ones (Li et al., 2017; Zhang et al., 2015). Computational Fluid Dynamics (CFD) tools, verified by measurement results, provide a useful tool in order to control and optimize NO_x reduction systems. They also enable better understanding of the phenomena occurring in furnaces. Most numerical analyses of the impact of air staging on the combustion process in large-scale boilers concern NO_x concentration in flue gases and the flue gas temperature. Their results show that air staging constitutes an effective way of reducing NO_x emissions. The OFA technology helps to reduce fuel consumption and thermal NO_x formation due to lessening the intensity of contact between the nitrogen contained in fuel and oxygen. The reduction in thermal NO_x on the other hand is related to the decrease in temperature in the combustion zone (Choi and Kim, 2009; Diez et al., 2008).

The OFA system efficiency depends primarily on the intensity of air and fuel mixing, the excess air ratio and the fuel particles' residence time. In general, the higher the intensity and the longer the residence time, the higher the efficiency (Biedermann et al., 2010). Yang et al. (2014) investigated the impact of staged combustion working parameters and fuel characteristic on the NO_x reduction efficiency. The obtained results show that the NO_x reduction rate increases as the residence time gets longer – in the case of high-volatile coal combustion, for the residence time from 0.8 to 2 s, the NO_x reduction rate rises from 20% to almost 75%. Moreover, the NO_x reduction rate increases also with a decrease in the excess air ratio λ : a drop in λ from 1.15 to 0.65 causes a 70% decrease in NO_x emissions. However, a further decrease in λ does not affect the reduction rate significantly (Yang et al., 2014).

Hwang et al. studied the effect of particle size on NO_x and unburnt carbon (UBC) emissions during air-staged combustion. Three particle sizes were taken into consideration (55, 75 and 95 μm). In general, the bigger the particle size, the higher the NO_x emissions and the lower the UBC content. If the fuel particle size is smaller, the particle specific surface area gets bigger. Due to that, the intensity of the contact between the fuel particles and combustion air increases, which results in a higher temperature of the particle and the combustion process is much faster (Hwang et al., 2016). Liu et al. conducted an analysis concerning mainly CO concentration in flue gases at various air-staged combustion levels differing in the burnt air ratio (the ratio of the amount of overfired air to the total amount of air) (Liu et al., 2016), whereas in (Liu et al., 2017) the authors focused on the aerodynamic field in a tangentially fired PF boiler in deep air-staged conditions.

Not much research has been carried out on the impact of changes in the location of OFA nozzles, the distribution of air to the nozzles or the air outflow angle on the combustion process in boilers with an air-staging system. This paper presents the results of studies concerning the effect of the above-mentioned parameters on the combustion process in a 230 t/h pulverized-coal (PC) boiler. The study was performed based on a numerical model created in the ANSYS Workbench package.

2. BOUNDARY CONDITIONS AND MODELING DESCRIPTION

Numerical investigations of the combustion process in the OP 230 boiler were carried out using the commercial program AnsysFluent. A numerical analysis of 11 variants of influence of air staging on the temperature of flue gas and emission of gases in the combustion chamber of the boiler was conducted. The OP

230 boiler is a two-pass drum boiler, fired with pulverized hard coal – Fig. 1. It has three step superheated steam, two air heaters and one water heater. The boiler is fired with 12 jet burners located in the corners of the furnace chamber. The boiler is supplied by 2 upper mills, each providing a pulverized-air mixture to 8 burners. The burners are enclosed in a common secondary air box. At the top of the furnace chamber eight OFA nozzles are located on two levels in the corners.

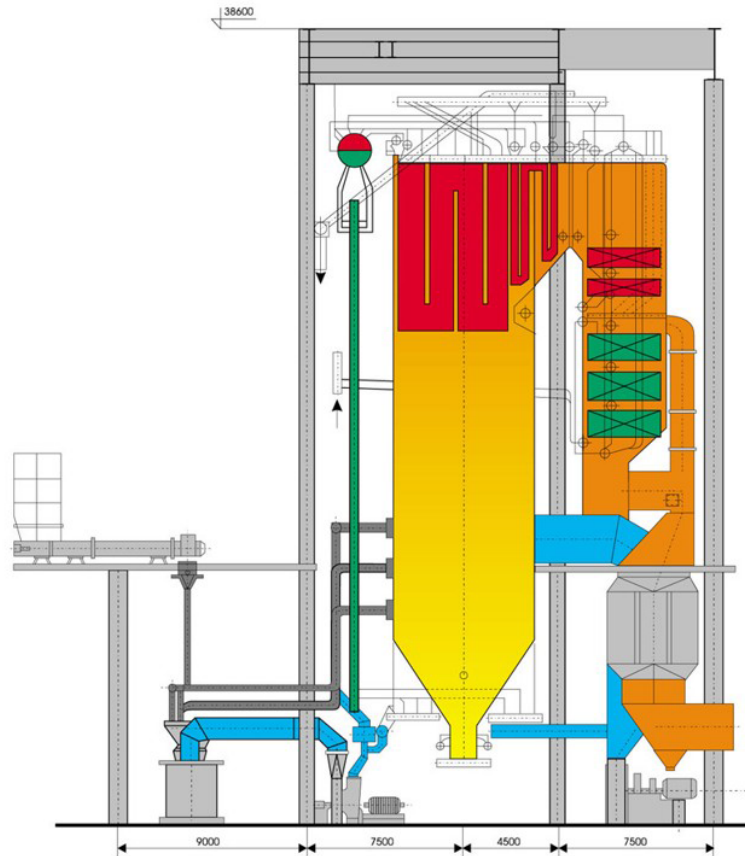


Fig. 1. Contour of the OP 230 boiler

Below in Table 1 coal properties (as received) are presented. The properties were the basis to develop input data for the CFD code.

Table 1. Coal properties (as received)

| Data | Symbol | Unit | Value |
|------------------|---------|-------|-------|
| Calorific value | Q_i^r | kJ/kg | 22692 |
| Ash content | A^r | % | 19.2 |
| Moisture content | W^r | % | 9 |
| Coal | C^r | % | 57 |
| Hydrogen | H^r | % | 4 |
| Sulphur | S^r | % | 1 |
| Oxygen | O^r | % | 9 |
| Nitrogen | N^r | % | 0.8 |

Table 2 presents the air and fuel mass flows implemented in the numerical code, and their temperatures. The following acronyms for corner descriptions were used: LF – left front, LR – left rear, RR – right rear, RF – right front.

Table 2. Air and fuel mass flow distribution with temperature

| Data | Unit | LF | LR | RR | RF |
|---------------------------|------|------|------|------|------|
| Primary air mass flow | kg/s | | | | |
| row 1 – bottom | | – | – | – | – |
| row 2 | | 2.25 | 2.27 | 2.25 | 2.24 |
| row 3 | | 2.25 | 2.26 | 2.27 | 2.27 |
| Coal mass flow | kg/s | | | | |
| row 1 – bottom | | – | – | – | – |
| row 2 | | 0.98 | 1 | 0.98 | 0.99 |
| row 3 | | 0.99 | 1.01 | 0.99 | 0.99 |
| Cooling air mass flow | kg/s | 1.36 | 1.37 | 1.35 | 1.33 |
| Secondary air mass flow | kg/s | 8.11 | 8.13 | 8.12 | 8.09 |
| Air mass flow to OFA | kg/s | | | | |
| row 1 | | 2 | 2.1 | 2.02 | 2 |
| row 2 | | 2 | 2 | 2 | 2.1 |
| Mixture temperature | K | 378 | | | |
| Secondary air temperature | | 543 | | | |

The geometrical model and the mesh composed of 505 519 numerical cells of the boiler are shown in Fig. 2. In the numerical model the combustion chamber, platen superheater and a small part of the second pass was included. The furnace chamber water walls are treated as flat surfaces exchanging heat with flue gases. The plate superheater is treated as porous media made of plates exchanging heat with flue gases. In order to simplify the creation of the numerical mesh, round-shaped burners have been simplified to rectangular-shaped burners with the same surface area – cf. Fig. 3.

Table 3 below shows the mesh quality indicators for the entire model. In order to simulate fuel combustion as accurately as possible, creating the best quality mesh within the combustion area was the main focus. The mesh outside the combustion area is of poorer quality.

Table 3. The mesh quality indicators

| | Minimum | Maximum | Average | Recommended value |
|-----------------|----------|---------|---------|-------------------|
| Aspect ratio | 1 | 25.3 | 2.6 | < 40 |
| Skewness | 0.000001 | 0.93 | 0.12 | < 0.8 |
| Element Quality | 0.07 | 0.99 | 0.65 | 0.75–1 |

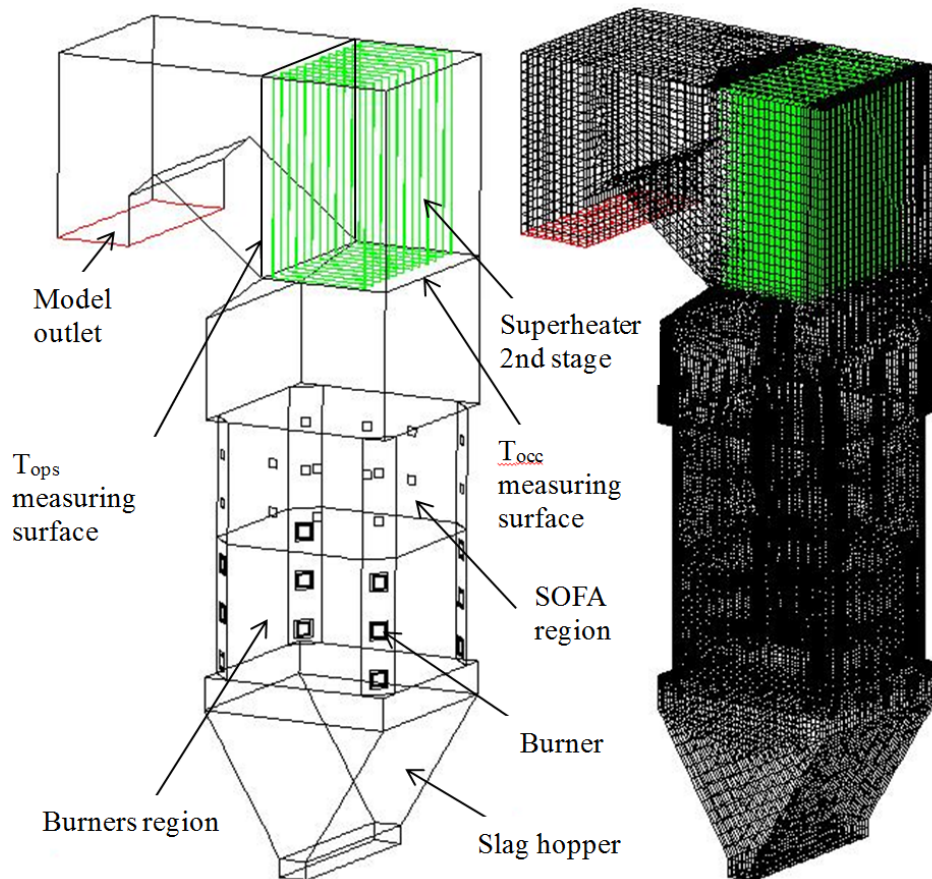


Fig. 2. The geometrical model and the numerical mesh of the boiler

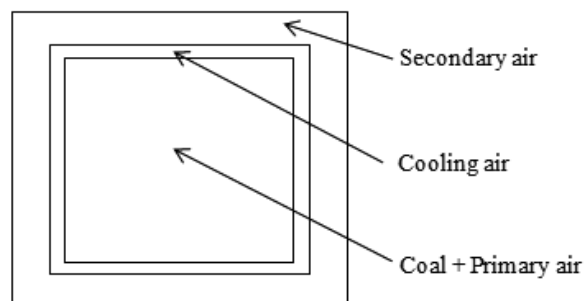


Fig. 3. The description of the rectangular-shaped burners

The SIMPLE method was used to estimate the flow fields (Choi and Kim 2009, Ibrahimoglu et al. 2016, Al-Abbas et al. 2013). The Euler-Lagrange two phase approach is more accurate than Euler-Euler approach in coal combustion modelling. The species transport model was used to simulate continuous phase. The Lagrange approach was used to determine the trajectories of the particle of the fuel in flue-gas. To simulate combustion of volatile fraction the Finite-Rate/Eddy-Dissipation model was used. This model allows one to control slower reaction in situations where the mixing process is intense, but the reaction should not occur. The heat exchange, mass and momentum, between the pulverized-coal particle and flue gas were computed using the Discrete Phase Model. Wet combustion model was used. The possibility of modelling devolatilization of coal and combustion of char is the greatest advantage of the two phase approach. Below one can see the reaction of oxidation of char to CO.



The Discrete Ordinates (DO) model was implemented to simulate the radiation between boiler furnace wall and coal particle surface. The emissivity and exchange of radiation between flue gas and particles was also modelled via DO model. The flue gas absorptivity was simulated by the grey gas model. The absorptivity is calculated based on the concentration of CO₂ and H₂O. The spherical shape of the fed fuel particles is assumed. The Rosin–Rammler–Sperling distribution is used. The concentration of NO was investigated using thermal and fuel nitrogen oxides. Table 4 presents the numerical model assumptions. Below, the reaction of the mechanism of the volatile fraction combustion and carbon monoxide oxidization is presented. The m, n, l, k, j coefficients were obtained based on coal composition according to volumetric reactions and using the Finite-Rate/Eddy-Dissipation model.

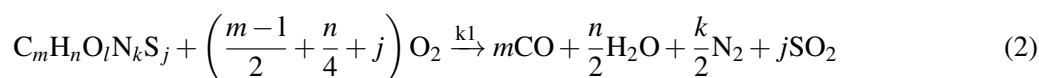


Table 4. Assumptions of the numerical model

| | |
|---|---|
| Two-phase model | Euler–Lagrange (Askarova et al., 2015; Choi and Kim, 2009; Diez et al., 2008; Sun et al. 2016; Zhang et al., 2015) |
| Turbulence model | Realizable k - ε (Askarova et al., 2015; Ibrahimoglu et al., 2016; Sun et al., 2016) |
| Combustion model | Finite-Rate/Eddy-Dissipation (Al-Abbas et al., 2013; Ibrahimoglu et al., 2016) |
| | Flue gas absorptivity: wsggm-domain-based model (Asotani et al., 2008; Choi and Kim, 2009; Ibrahimoglu et al., 2016; Sun et al. 2016) |
| For the coal particle the following was assumed | |
| Devolatilization | Single Rate model (Asotani et al., 2008; Zhang et al., 2009) |
| Combustion of char | The kinetic-diffusion model (Choi and Kim, 2009; Sun et al., 2016) |
| Radiation model | DO (Choi and Kim, 2009; Ibrahimoglu et al., 2016; Zhang et al., 2009) Flow Iterations per radiation iteration: 1 Theta divisions: 4 Phi divisions: 4 Theta pixels: 3 Phi pixels: 3 |

The reactions and the constants adopted in the numerical model made it possible to obtain results which are similar to the 0-dimensional model of the boiler – cf. Table 5 where the model validation for calculations was showed.

Table 5. Model validation for calculations

| Data | Unit | CKTI | CFD |
|------------------|------|------|------|
| O ₂ | % | 3.26 | 2.62 |
| T _{occ} | K | 1418 | 1424 |
| T _{ops} | K | 1098 | 1120 |

The air staging was carried out by adding eight OFA nozzles on the two opposing walls (nozzles in the corners will be called corner nozzles and nozzles on the walls will be called wall nozzles). The location of the OFA nozzles is shown in Fig. 4.

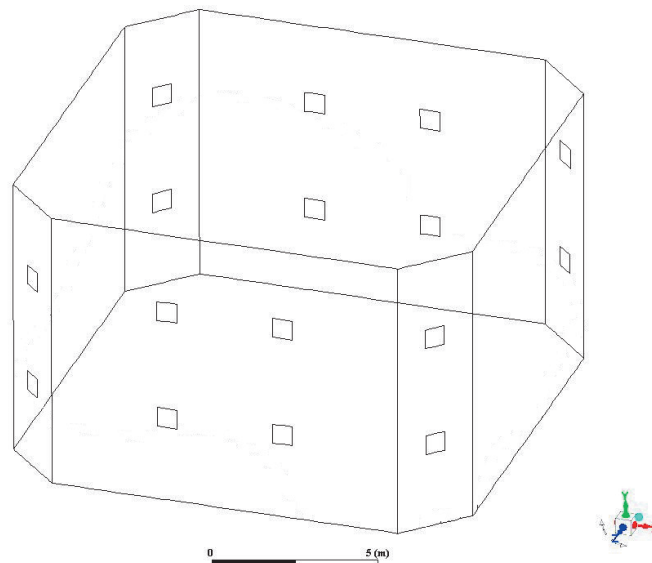


Fig. 4. The location of the OFA nozzles in OFA region

In the paper the analysis of 11 cases of air staging was presented:

- Case 1. The whole air was fed through the burners (the air from OFA nozzle was evenly added to cooling and secondary air).
- Case 2. The air from the corner nozzles is fed at the same angle as the fuel and the air from the burners – 40°C angle. Base case – working on the real boiler.
- Case 3. The air from the wall nozzles is supplied at an angle of 90°C.
- Case 4. The air from the wall nozzles is supplied at an angle of 80°C.
- Case 5. The air from the wall nozzles is supplied at an angle of 70°C.
- Case 6. Air from wall nozzles, one nozzle at an angle of 60°C, the other – 70°C.
- Case 7. Air in the first level is supplied from the corner nozzles – angle 40°C, the air at the second level is fed from the wall nozzles at an angle of 70°C.
- Case 8. Air in the first level is supplied from the corner nozzles – angle 40°C, the air at the second level is fed from the wall nozzles at an angle of 110°C.
- Case 9. Air in the first level is supplied from the corner nozzles – angle 40°C, the air at the second level is fed from the wall nozzles at an angle of 120°C.
- Case 10. Air in the first level is supplied from the corner nozzles – angle 50°C, the air at the second level is fed from the wall nozzles at an angle of 70°C.
- Case 11. Air from wall nozzles, one nozzle at an angle of 100°C, the other – 110°C.

To illustrate the multivariate nature of numerical studies in Figures 5 to 9, the mass fraction of oxygen in the planes passing through the two OFA nozzles level and the second level of the burners are shown.

Case 1 was used to verify the model, because the CKTI method does not take into account the use of air staging. In the validation of the model used for calculations, the focus was on fitting the O₂ fraction in the flue-gas, the temperature of the flue-gas at the outlet of the combustion chamber T_{occ} and the temperature of the flue-gas behind the plate superheater T_{ops} .

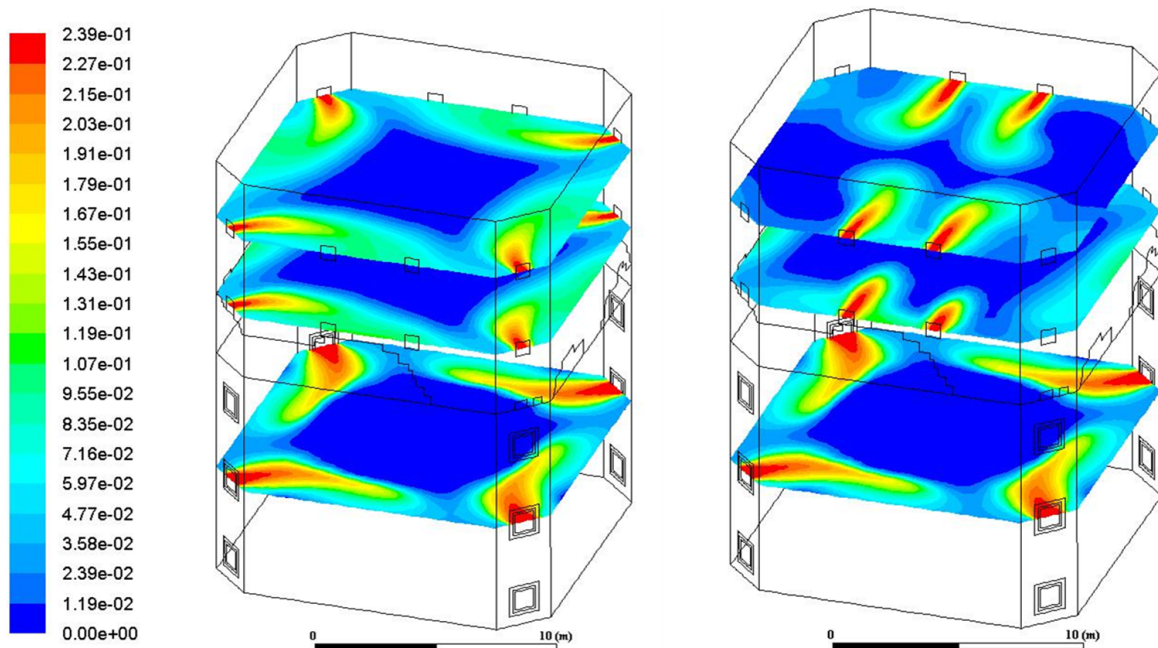


Fig. 5. The mass fraction of oxygen for Case 2 (on the left) and Case 3 (on the right)

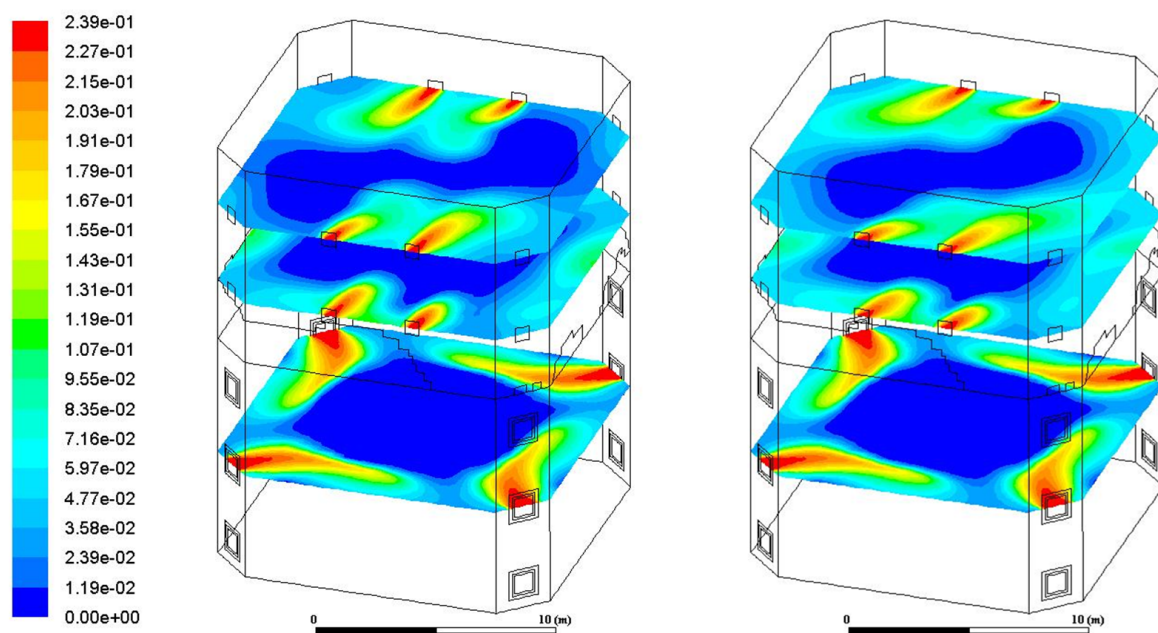


Fig. 6. The mass fraction of oxygen for Case 4 (on the left) and Case 5 (on the right)

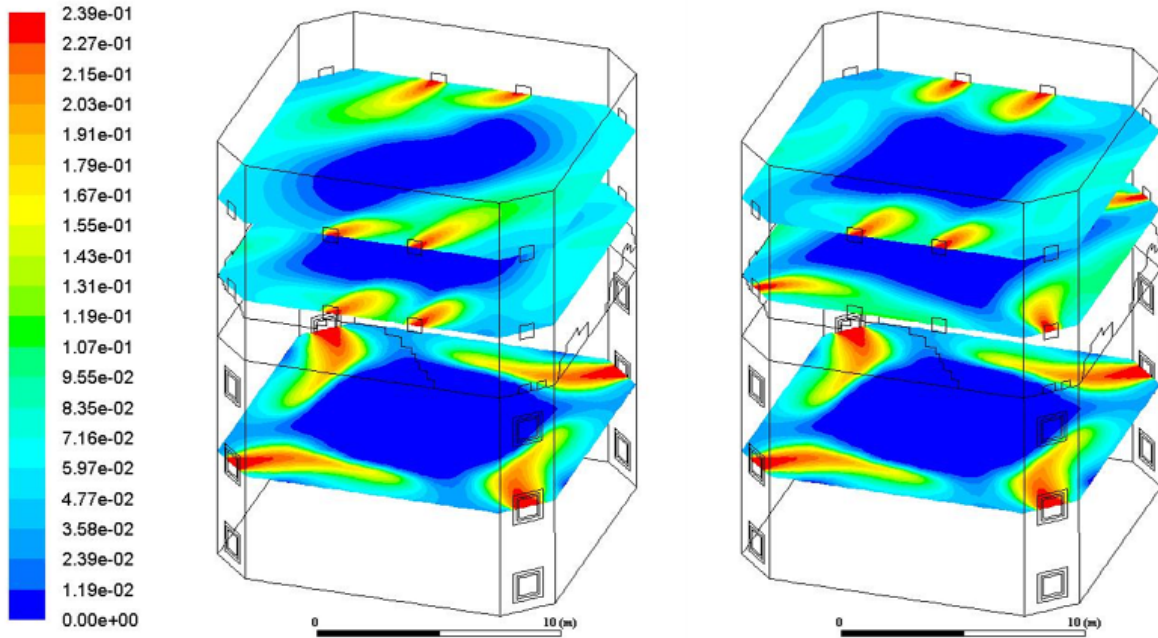


Fig. 7. The mass fraction of oxygen for Case 6 (on the left) and Case 7 (on the right)

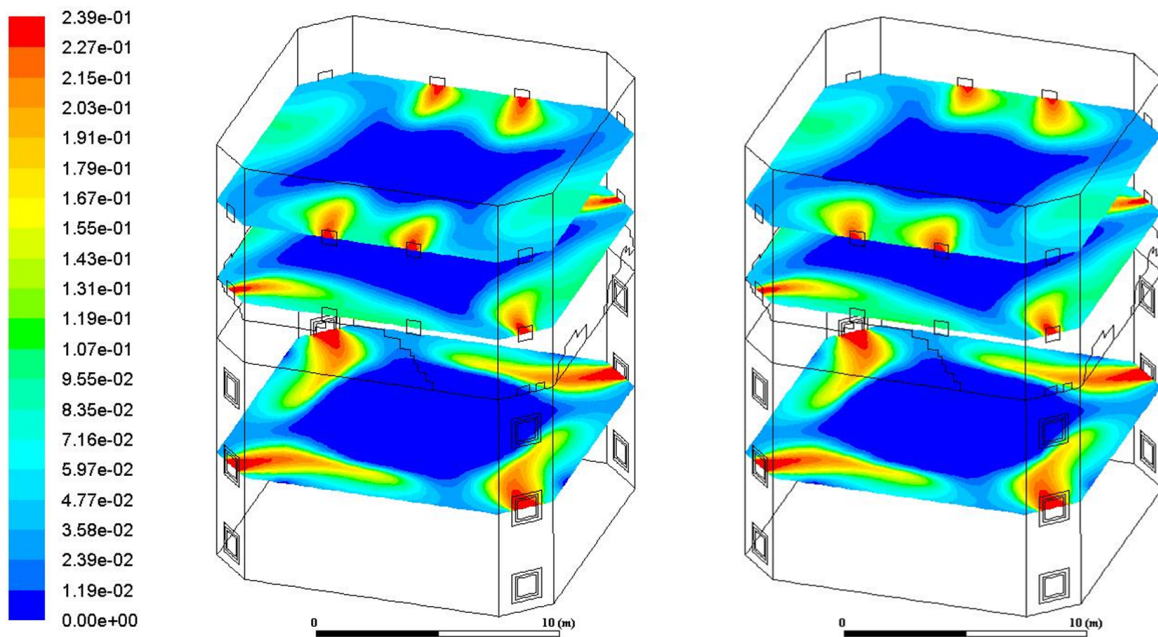


Fig. 8. The mass fraction of oxygen for Case 8 (on the left) and Case 9 (on the right)

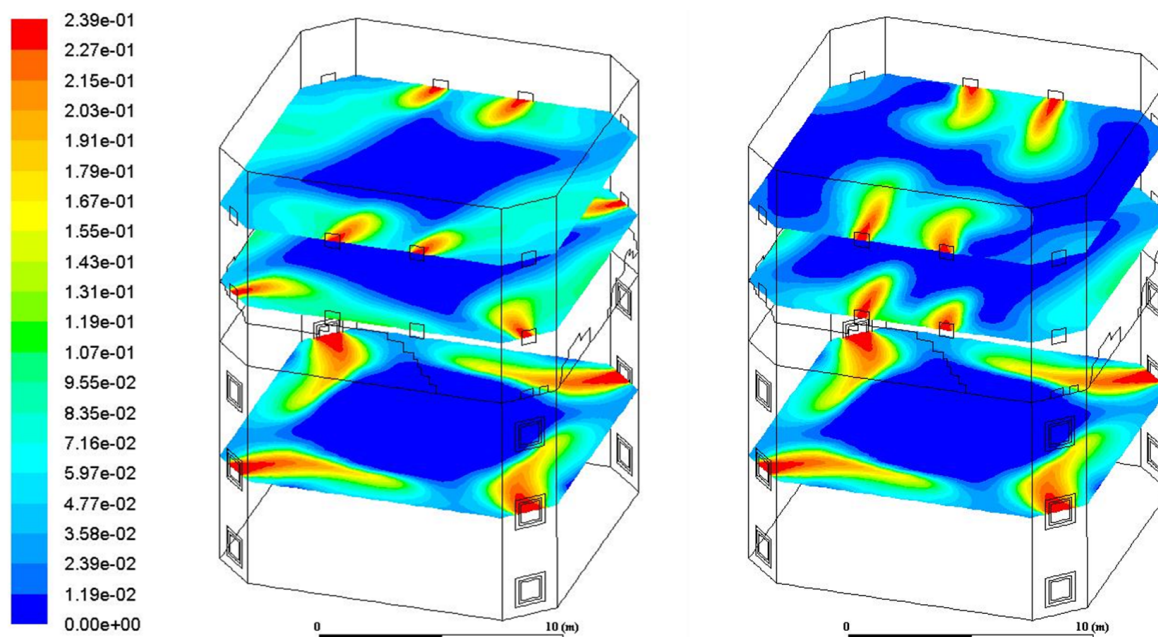


Fig. 9. The mass fraction of oxygen for Case 10 (on the left) and Case 11 (on the right)

3. RESULTS WITH ANALYSIS

Table 6 shows the percentage composition of the flue-gas at the outlet of the model, the temperature of the flue-gas at the outlet of the combustion chamber T_{occ} , the temperature of the flue-gas behind the platen superheater T_{ops} and the percentage of the fuel stream directed towards the slag hopper M_{sh} . It also converted the amount of nitrogen oxides to flue-gas containing 6% oxygen.

Table 6. The results of all simulations

| Case | O ₂ | SO ₂ | CO | NO _x | T_{occ} | T_{ops} | M_{sh} |
|------|----------------|-----------------|--|--|-----------|-----------|----------|
| | % | % | mg/m ³ , 6% O ₂ | mg/m ³ , 6% O ₂ | K | K | % |
| 1 | 2.62 | 0.22 | 114.2 | 593.0 | 1424.1 | 1119.2 | 0.180 |
| 2 | 2.85 | 0.22 | 280.8 | 432.6 | 1421.5 | 1131.7 | 0.260 |
| 3 | 2.93 | 0.22 | 10.4 | 429.4 | 1370.2 | 1049.8 | 0.475 |
| 4 | 2.81 | 0.22 | 36.1 | 428.3 | 1387.9 | 1073.4 | 0.516 |
| 5 | 2.75 | 0.22 | 90.4 | 440.4 | 1420.6 | 1112.3 | 0.296 |
| 6 | 2.78 | 0.22 | 196.4 | 429.6 | 1425.2 | 1138.7 | 0.334 |
| 7 | 2.86 | 0.22 | 162.2 | 429.5 | 1438.7 | 1128.2 | 0.491 |
| 8 | 2.78 | 0.22 | 46.3 | 436.0 | 1409.5 | 1095.1 | 0.385 |
| 9 | 2.69 | 0.22 | 94.2 | 425.5 | 1411.4 | 1109.9 | 0.364 |
| 10 | 2.84 | 0.22 | 115.6 | 432.4 | 1437.4 | 1122 | 0.361 |
| 11 | 2.93 | 0.22 | 10.4 | 420.9 | 1358.4 | 1040.6 | 0.621 |

Below, the emission of carbon monoxide and nitrogen oxides at the outlet of the model was shown (Fig. 10).

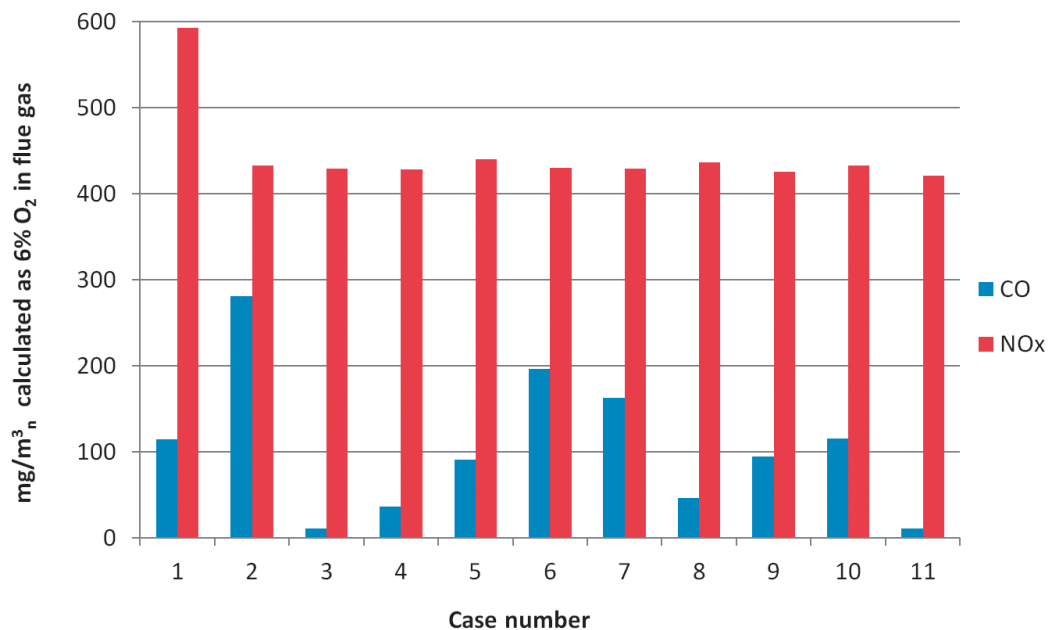


Fig. 10. Comparison of carbon monoxide and nitrogen oxide emissions

The use of OFA nozzles (cases 2–11) results in a reduction of NO_x in the flue-gas by about 150 mg/m^3 compared to combustion without OFA nozzles (case 1). The manipulation of the angle and location of the OFA nozzles causes no change in NO_x in the flue-gas, but causes a change in the amount of CO. In cases in which the vortex created in the combustion chamber is affected, the reduction of CO in the flue-gas occurred. The highest reduction of carbon monoxide occurs in cases 3, 4, 8 and 11 where the combustion vortex was most affected. This results in better mixing of flue-gas components and carbon monoxide burnout. For cases without interruption of vortex (cases 2, 5, 6, 7) or with vortex partially recovered (cases 5, 6, 9, 10), the CO fraction in the flue-gas was significantly higher. Case 3 where the delivery of OFA air takes place on boiler walls, perpendicular to the surface of the nozzles as well as case 11 where slight deviation from the right angle occurs results in a reduction of CO to the level of $10 \text{ (mg/m}^3)$. Due to better mixing, the equalization of the concentrations of components of flue-gas and burnout of the combustible particles is improved. In cases from 4 to 6, wall nozzles were used again to restore the vortex of combustion within the OFA region. The angular deviation changed from 80 to 60 degree caused partial recovery of the vortex and increased CO in the flue-gas. In cases 7–10 the angle of air at the second level of OFA nozzles was changed and on the first level of OFA the air was fed through corner nozzles. This has affected the change in CO emissions.

Figure 11 shows the temperature at the outlet of the combustion chamber for all 11 cases. Disruption of combustion vortex (variants 3, 4, 8, 9, 11) causes a significant reduction of the temperature of flue-gas.

The highest temperature of the flue-gas was achieved in case 7, where the first level of the OFA nozzles worked at corners and the second level of OFA nozzles used wall nozzles (assisted in the vortex creation). The lowest temperature of the flue-gas was obtained for case 3, where the air is fed from the wall OFA nozzles.

Figure 12 shows the percentage of the fuel stream directed towards the slag hopper M_{sh} , which consists of burnt and unburned particles. Vortex disturbance (cases 3, 4, 7, 11) causes an increase of the falling coal stream towards the slag hopper to 0.62% of all coal particles in the combustion chamber.

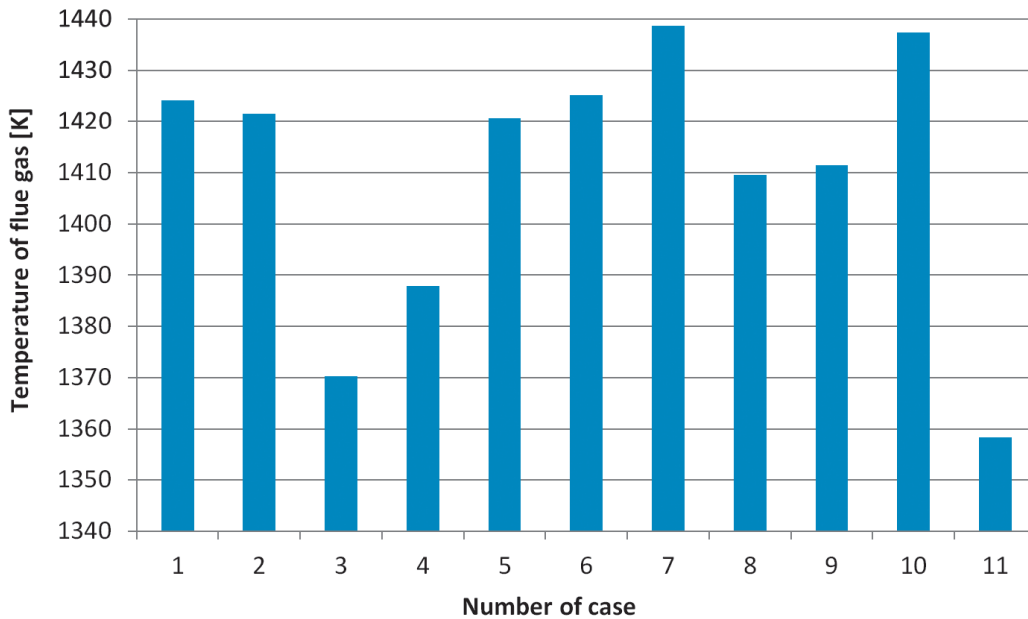


Fig. 11. The temperature at the outlet of the combustion chamber

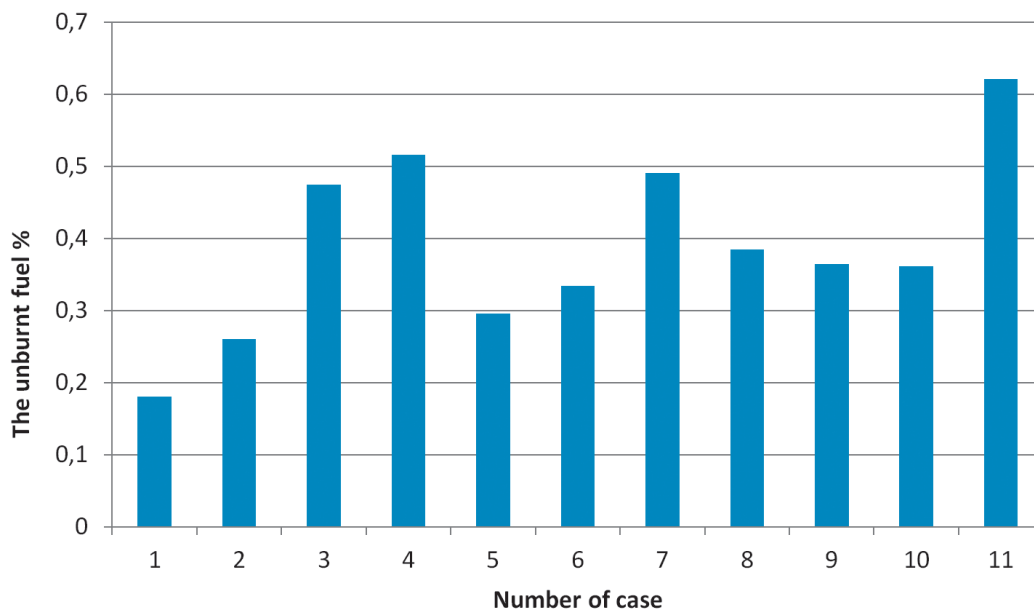


Fig. 12. Chart of the change of the particle stream

The contour of the temperature of flue-gas at the outlet of the combustion chamber was shown in Figs 13–17.

The air staging changes the contour of the temperature of flue-gas at the outlet of the combustion chamber. For the base case 2 with the existing combustion vortex, the highest temperature is localized at the centre of the outlet surface of the combustion chamber, while in case of the interrupted vortex (case 3 – Fig. 13 and case 11 – Fig. 17) the temperature is lower and its contour is more uniform at the outlet surface. The attempt to reconstruct the vortex with the wall nozzles (case 4, 5, 6 – Figs 14, 15) results in occurrence of areas of higher temperature and uneven elliptical shape.

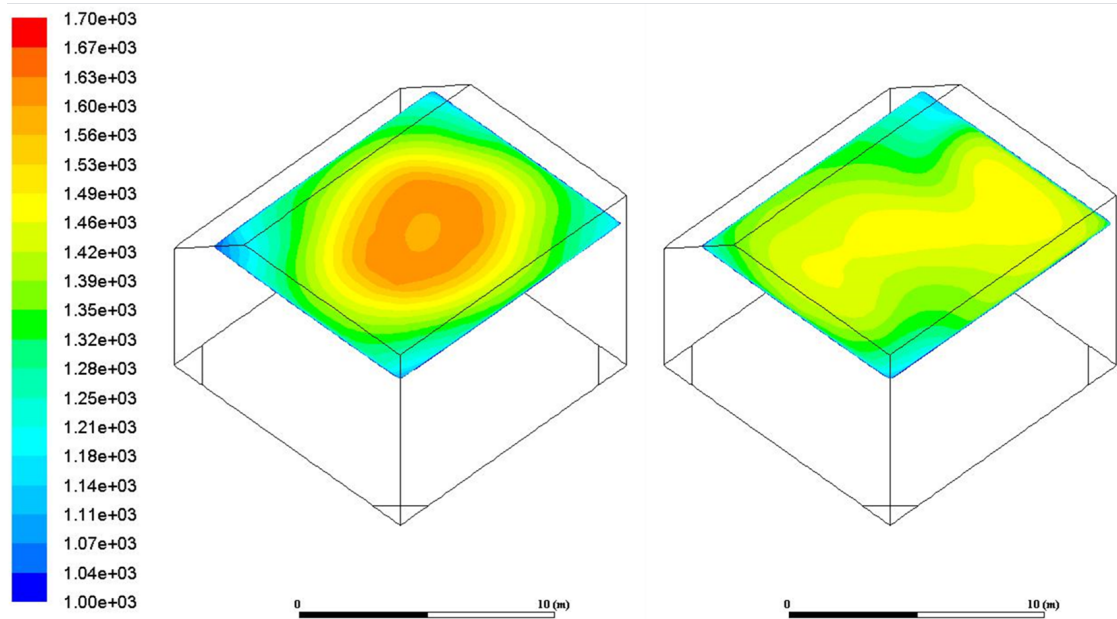


Fig. 13. Contour of the temperature of flue-gas at the outlet of the combustion chamber [K] case 2 (on the left) and case 3 (on the right)

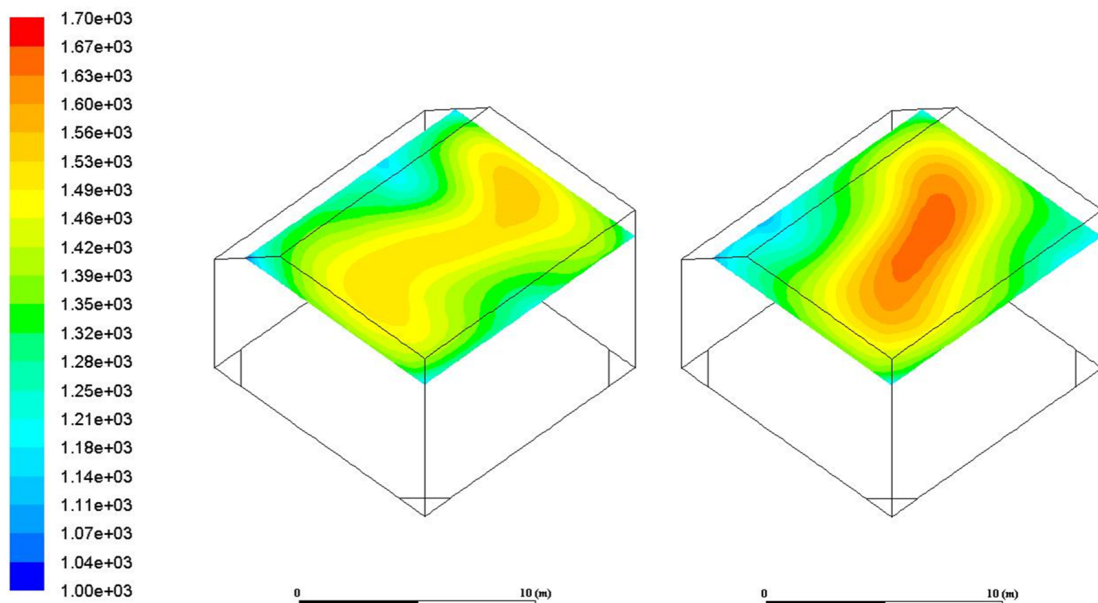


Fig. 14. Contour of the temperature of flue-gas at the outlet of the combustion chamber [K] case 4 (on the left) and case 5 (on the right)

For proper operation of the platen superheater, a uniformly and aligned flue-gas profile in front of it is required. In that case the superheater tubes are uniformly heat-loaded and the temperature spread of steam across the superheater's degree was reduced. Thus, for platen superheater cases 3 and 11 are most preferred.

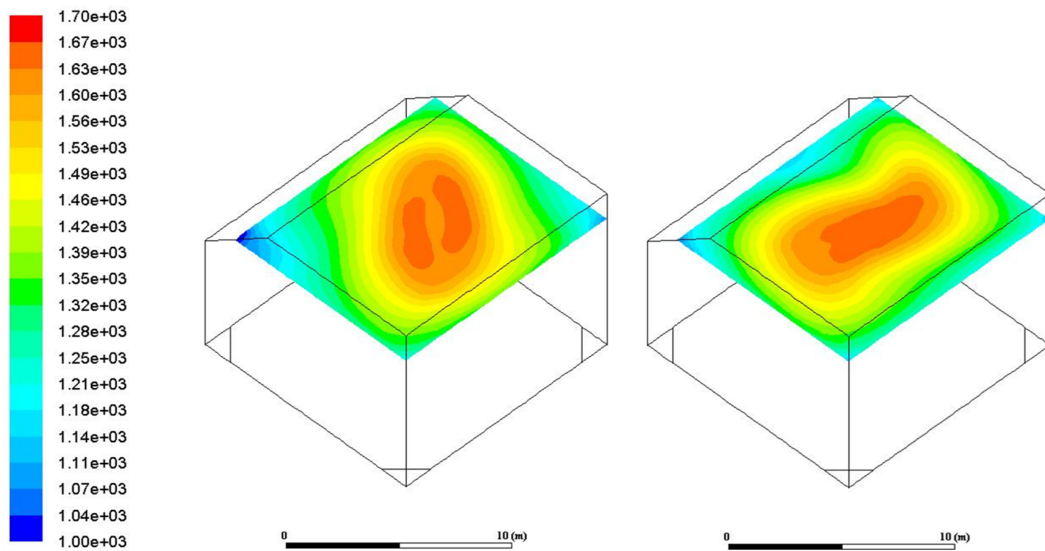


Fig. 15. Contour of the temperature of flue-gas at the outlet of the combustion chamber [K] case 6 (on the left) and case 7 (on the right)

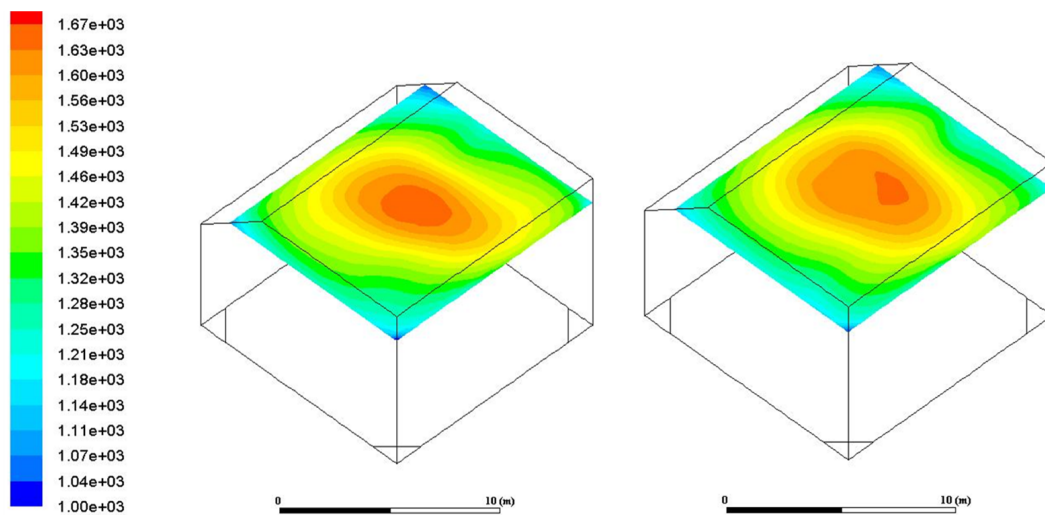


Fig. 16. Contour of the temperature of flue-gas at the outlet of the combustion chamber [K] case 8 (on the left) and case 9 (on the right)

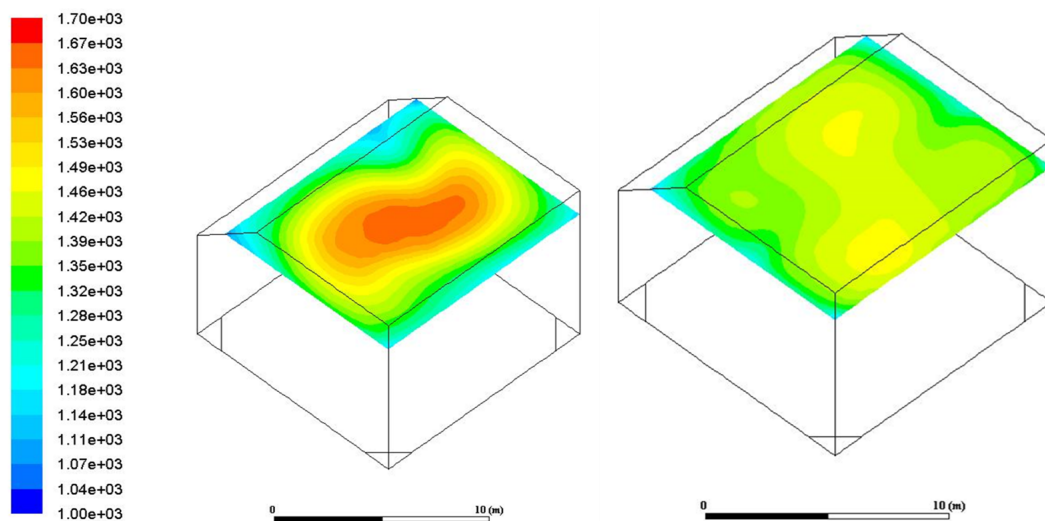


Fig. 17. Contour of the temperature of flue-gas at the outlet of the combustion chamber [K] case 10 (on the left) and case 11 (on the right)

4. CONCLUSIONS

- The use of OFA nozzles significantly reduces emissions of NO_x with identical combustion parameters.
- Changing the angle in horizontal plane of the air supply from the OFA nozzles does not affect NO_x emissions (cases 2–11).
- Changing the place of the OFA nozzles at the same height does not affect the emission of nitrogen oxides (cases 3–6 and 7–10).
- Interruption of the vortex (cases 3, 4, 8, 11) in the combustion chamber decreases CO content in flue-gas at the outlet of the combustion chamber and increases the fuel stream directed towards the slag hopper.
- Interruption of the vortex (cases 3, 11) equalizes the profile of the temperature of the flue-gas on the outlet of the combustion chamber.
- For proper operation of the platen superheater, a uniformly and aligned flue-gas profile in front of it is required. Thus, for platen superheater cases 3 and 11 are most preferred.
- Different types of air staging without having to build areal configuration to find the best and most optimal solutions could be realized with numerical methods.

Investigations presented in this work were partially financed within the design and modernization tasks of the basic node of machinery and power equipment BK/287/RIE5/2017/502.

REFERENCES

- Al-Abbas A.H., Naser J., Hussein E.K., 2013. Numerical simulation of brown coal combustion in a 550 MW tangentially-fired furnace under different operating conditions. *Fuel*, 107, 688–698. DOI: 10.1016/j.fuel.2012.11.054.
- Askarova A., Bolegenova S., Maximov V., Beketayeva M., Safarik P., 2015. Numerical modelling of pulverized coal combustion at thermal power plant boilers. *J. Thermal Sci.*, 24, 275–282. DOI: 10.1007/s11630-015-0784-0.
- Asotani T., Yamashita T., Tominaga H., Uesugi Y., Itaya Y., Mori S., 2008. Prediction of ignition behaviour in a tangentially fired pulverized coal boiler using CFD. *Fuel*, 87, 482–490. DOI: 10.1016/j.fuel.2007.04.018.
- Biedermann F., Brunner T., Obernberger I., Sippula O., Boman Ch., Ohman M., Bafer L., 2010. *Summary and evaluation of existing data on air staging strategies* – Project ERA-NET “Future BioTex” Report.
- Buchmayr M., Gruber J., Hargassner M., Hochenauer C., 2016. A computationally inexpensive CFD approach for small-scale biomass burners equipped with enhanced air staging. *Energy Convers. Manage.*, 115, 32–42. DOI: 10.1016/j.enconman.2016.02.038.
- Carroll J.P., Finnan J.M., Biedermann F., Brunner T., Obernberger I., 2015. Air staging to reduce emissions from energy crop combustion in small scale applications. *Fuel*, 155, 37–43. DOI: 10.1016/j.fuel.2015.04.008.
- Choi C.R., Kim C.N., 2009. Numerical investigation on the flow, combustion and NO_x emission characteristics in a 500MWe tangentially fired pulverized-coal boiler. *Fuel*, 88, 1720–1731. DOI: 10.1016/j.fuel.2009.04.001.
- Diez L.I., Cortes C., Pallares J., 2008. Numerical investigation of NO_x emissions from a tangentially-fired utility boiler under conventional and overfire air operation. *Fuel*, 87, 1259–1269. DOI: 10.1016/j.fuel.2007.07.025.
- Directive 2010/75/EU of the European Parliament and the Council on industrial emissions.
- Hardy T., Pawlak-Kruczek H., 2017. Reburning: An efficient method for reduction of NO_x in boilers steam. Available at: <http://www.spalanie.pwr.edu.pl/badania/publikacje/reburning%20skuteczna%20metoda.PDF> (in Polish).
- Hwang M.-Y., Ahn S.-G., Jang H.-C., Kim G.-B., Jeon C.-H., 2016. Numerical study of an 870MW wall-fired boiler using De- NO_x burners and an air staging system for low rank coal. *J. Mech. Sci. Technol.*, 30, 5715–5725. DOI: 10.1007/s12206-016-1142-1.

- Ibrahimoglu B., Yilmazoglu M. Z., Cucen A., 2016. Numerical modelling of repowering of a thermal power plant boiler using plasma combustion systems. *Energy*, 103, 38–48. DOI: 10.1016/j.energy.2016.02.130.
- Khodaei H., Guzzomi F., Yeoh G. H., Regueiro A., Patino D., 2017. An experimental study into the effect of air staging distribution and position on emissions in a laboratory scale biomass combustor. *Energy*, 118, 1243–1255. DOI: 10.1016/j.energy.2016.11.008.
- Kuang M., Li Z., Liu C., Zhu Q., 2013. Experimental study on combustion and NO_x emissions for a down-fired supercritical boiler with multiple-injection multiple-staging technology without overfire air. *Appl. Energy*, 106, 254–261. DOI: 10.1016/j.apenergy.2013.01.072.
- Li S., Chen Z., He E., Jiang B., Li Z., Wang Q., 2017. Combustion characteristics and NO_x formation of a retrofitted low-volatile coal-fired 330 MW utility boiler under various loads with deep-air-staging. *Appl. Therm. Eng.*, 110, 223–233. DOI: 10.1016/j.applthermaleng.2016.08.159.
- Liu Y., Fan W., Li Y., 2016. Numerical investigation of air-staged combustion emphasizing char gasification and gas temperature deviation in a large-scale, tangentially fired pulverized-coal boiler. *Appl. Energy*, 177, 323–334. DOI: 10.1016/j.apenergy.2016.05.135.
- Liu Y.C., Fan W.D., Wu M.Z., 2017. Experimental and numerical studies on the gas velocity deviation in a 600 MWe tangentially fired boiler. *Appl. Therm. Eng.*, 110, 553–563. DOI: 10.1016/j.applthermaleng.2016.08.185.
- Nussbaumer T., 1997. Primary and secondary measures for the reduction of nitric oxide emissions from biomass combustion. *Dev. Thermochem. Biomass Convers.*, 1447–1461. DOI: 10.1007/978-94-009-1559-6_113.
- Spliethoff H., Greul U., Rudgier H., Hein K.R.G., 1996. Basic effects on NO_x emissions in air staging and reburning at a bench-scale test facility. *Fuel*, 75, 560–564. DOI: 10.1016/0016-2361(95)00281-2.
- Sun W., Zhong W., Yu A., Liu L., Qian Y., 2016. Numerical investigation on the flow, combustion, and NO_x emission characteristics in a 660 MWe tangential firing ultra-supercritical boiler. *Adv. Mech. Eng.*, 8, 1–13. DOI: 10.1177/1687814016630729.
- Yang J., Sun R., Sun S., Zhao N., Hao N., Chen H., Wang Y., Guo H., Meng J., 2014 Experimental study on NO_x reduction from staging combustion of high volatile pulverized coals. Part 1. Air staging. *Fuel Process. Technol.*, 126, 255–275. DOI: 10.1016/j.fuproc.2014.04.034.
- Zhang X., Zhou J., Sun S., Sun R., Qin M., 2015. Numerical investigation of low NO_x combustion strategies in tangentially-fired coal boilers. *Fuel*, 142, 215–221. DOI: 10.1016/j.fuel.2014.11.026.

Received 09 November 2017

Received in revised form 15 January 2018

Accepted 05 February 2018